Brief note

Struct Multidisc Optim 28, 221–227 (2004)
DOI 10.1007/s00158-004-0403-2

Structural shape optimisation using boundary elements and the biological growth method

C. Wessel, A. Cisilino and B. Sensale

Abstract A numerical evolutionary procedure for the structural optimisation for stress reduction of two-dimensional structures is presented in this paper. The proposed procedure couples the biological growth method (BGM) with the boundary element method (BEM). The boundary-only intrinsic characteristic of BEM together with its accuracy in the boundary displacement and stress solutions make BEM especially attractive for solving shape-optimisation problems. Two formulations of BEM are used in this work: the standard for two-dimensional elastostatics for the stress analysis and the dual reciprocity method (DRM), which is used to model the swelling or shrinking of the material. Two examples are analysed to illustrate the proposed methodology and to demonstrate its versatility and robustness.

Key words biological growth method, boundary elements method, dual reciprocity method, shape optimisation

1 Introduction

The failure of structures under service conditions frequently takes place at highly stressed points. Therefore, it is crucial for designers to avoid stress peaks in order to maximise a component service life, a fact that justifies the importance given to the subject so far. The deterministic strategies for the solution of the structural optimisation problems are, on the one hand, the mathematical programming methods and, on the other, the optimality criterion-based methods.

In the former, well-established mathematical tools are used, like direct search (Trosset 1997), derivative-free methods (Lucidi *et al.* 2002; Lewis *et al.* 2000) and gradientless methods (Schnack 1988; Schnack *et al.* 1988; Iancu and Schnack 1989; Schnack and Iancu 1989).

The latter, that is, optimality criterion-based methods, take advantage of the knowledge on the physics and mechanics of the particular problem (Sauter *et al.* 1996), providing a necessary condition for a minimum of the objective function. The physical and mechanical knowledge put to use in optimality criterion-based methods is also their principal drawback, as it limits their application to certain definite areas.

Biological structures, such as bones and trees, provide a simple example for shape optimisation, as they change their contour to adapt to external loads while reducing stress peaks. In this line, Mattheck (1990) introduced an optimality criterion method called the biological growth method (BGM), related to Schnack's gradientless method (Iancu 1991; Schnack *et al.* 1988; Spörl 1985; Schnack 1978). Based on his observations in Nature, Mattheck posits that biological structures always self-optimise their geometry to attain a state of constant stress at part of or the whole of the surface of the structure. The process of self-optimisation is carried out through the swelling or shrinking of the soft outermost layer of material, which yields the levelling of local stresses.

Since the original work by Mattheck and Burkhardt (1990) was published, some papers have appeared coupling the BGM with the finite element method (FEM) for structural shape optimisation (Chen and Tsai 1993; Sauter 1993; Tekkaya and Güneri 1998). At the same time, the boundary element method (BEM) has become a popular alternative in structural shape optimisation (Baron and Yang 1988; Kane and Saigal 1988; Mellings and Aliabadi 1995) due to its accuracy in the boundary displacement and stress solutions, as well as the fact that remeshing is simpler for BEM than for FEM.

Received: 26 June 2002
Revised manuscript received: 28 January 2004
Published online: 6 July 2004

C. Wessel[1, ✉], A. Cisilino[2] and B. Sensale[3]

[1] Facultad de Ingeniería, Universidad Austral, Garay 125, Ciudad Autónoma de Buenos Aires, Argentina
e-mail: cwessel@fi.mdp.edu.ar
[2] Facultad de Ingeniería, Universidad Nacional de Mar del Plata – CONICET, Av. Juan B. Justo 4302 (7600) Mar del Plata, Argentina
[3] Instituto de Estructuras y Transporte, Facultad de Ingeniería, Universidad de la República, J. Herrera y Reissig 665 – 11300 Montevideo, Uruguay

These intrinsic characteristics of BEM, together with the idea behind BGM that the swelling of the soft outermost layer of material governs the optimisation process, make BEM especially attractive for solving shape-optimisation problems using Mattheck's approach. To the authors' knowledge, there is only one published paper dedicated to coupling BGM and BEM, i.e., Cai *et al.* (1998). However, in that work, the authors extended the swelling of the material to the complete model domain, not only to the boundary layer as proposed by Mattheck.

The swelling of the soft, thin, outermost layer of material is modelled in the present work by using the so-called dual reciprocity formulation of the BEM. The implementation proposed in this work, then, makes use of two BEM formulations: the standard for two-dimensional elastostatics, which is used for the stress analysis of the problem; and dual reciprocity method (DRM) to model swelling. Both formulations are coupled in an evolutionary algorithm. Splines provide the model remeshing. The algorithm is presented in this paper together with two examples that illustrate the methodology and demonstrate its versatility and robustness.

2 The biological growth method

The biological growth method (BGM) was first introduced by Mattheck (1990). Based on his observations of nature (tree butts, branch joints, deer antlers, etc.), he proposed that biological structures always self-optimise their shapes according to natural external loads. He defined *optimum shape* as the one that shows a state of constant stress at part of or the whole of the surface of the component. The process of self-optimisation consists in the swelling or the shrinking of the soft, outermost layer of material, following the law

$$\dot{\varepsilon}_v = k\,(\sigma_{vm} - \sigma_{ref})\,, \tag{1}$$

where $\dot{\varepsilon}_v$ is the volumetric swelling strain rate, which is stated to be proportional to a driving function given by the difference between von Mises stress (σ_{vm}) and a reference stress (σ_{ref}), an expected value.

Equation (1) holds for each point in the optimisation domain. It simply expresses the fact that, for each point, if the von Mises stress is bigger than the reference stress ($\sigma_{vm} - \sigma_{ref} > 0$), the thin layer swells, while, if the von Mises stress is lower than the reference stress ($\sigma_{vm} - \sigma_{ref} < 0$), the thin layer shrinks.

An elegant method to implement (1) is by means of a thermal expansion, as described by Tekkaya and Güneri (1998). After applying an Euler integration scheme to (1) for a time span of Δt, the volumetric swelling strain can be expressed as

$$\varepsilon_v = k(\sigma_{vm} - \sigma_{ref})\Delta t \tag{2}$$

Besides, the generalised Hooke's law is given by

$$\begin{aligned}
\varepsilon_x &= \frac{1}{E}\left[\sigma_x - \nu(\sigma_y + \sigma_z)\right] + \alpha\theta \\
\varepsilon_y &= \frac{1}{E}\left[\sigma_y - \nu(\sigma_x + \sigma_z)\right] + \alpha\theta \\
\varepsilon_y &= \frac{1}{E}\left[\sigma_z - \nu(\sigma_x + \sigma_y)\right] + \alpha\theta\,,
\end{aligned} \tag{3}$$

where ε_x, ε_y and ε_y are the normal infinitesimal strain components, σ_x, σ_y and σ_z are the normal components of the Cauchy stress tensor, ν is the Poisson ratio, α is the thermal expansion coefficient, E is the Young modulus and θ is the temperature field. Now, if E is reduced considerably in the optimisation domain, as proposed by Mattheck, mechanical strains can be neglected even if the boundary conditions of the real problem are kept, so that

$$\varepsilon_x \approx \varepsilon_y \approx \varepsilon_z \approx \alpha\theta\,. \tag{4}$$

If the thermal expansion is only defined to be nonzero in the optimisation domain, then, in that particular zone,

$$\varepsilon_{sw} = \alpha\theta\,. \tag{5}$$

Considering that both σ_{vm} and θ are functions of position, the comparison of (2) and (5) gives

$$\begin{aligned}
&\Delta t \Leftrightarrow \alpha \\
&k(\sigma_{vm} - \sigma_{ref}) \Leftrightarrow \theta\,.
\end{aligned} \tag{6}$$

Consequently, (1) can be expressed as

$$\alpha\theta = \gamma k(\sigma_{vm} - \sigma_{ref})\,, \tag{7}$$

where γ is a units conversion factor.

Special attention should be taken to choose suitable values of σ_{ref}. Otherwise, and as pointed out by Mattheck and Moldenhauer (1990), the whole process of optimisation may not converge.

3 The boundary element method

In what follows, a brief description of the boundary element method (BEM) is given in order to point out the different formulations used in this work. For further details on BEM, the reader should refer to the books by Brebbia and Dominguez (1992) and Partridge *et al.* (1992).

3.1 BEM for two-dimensional elasticity

The starting point of the formulation of BEM for two-dimensional elasticity is the Navier equation,

$$G u_{j,kk} + \frac{G}{1-2\nu} u_{k,kj} + b_j = 0\,, \tag{8}$$

where j, k denote Cartesian components, G is the shear modulus, b_j are the components of body forces and u_k are the displacements.

Following Brebbia and Dominguez (1992), the corresponding boundary integral equation for a domain $\Omega(x)$ confined by the boundary surface $\Gamma(x)$ is

$$c^i_{lk}(x')u^i_k(x') + \int_\Gamma p^*_{lk}(x',x)u_k(x)\,\mathrm{d}\Gamma(x) =$$

$$\int_\Gamma u^*_{lk}(x',x)p_k(x)\,\mathrm{d}\Gamma(x) + \int_\Omega u^*_{lk}(x',x)b_k(x)\,\mathrm{d}\Omega(x)\,, \qquad (9)$$

where $u^*_{lk}(x',x)$ is the fundamental solution of (8) and $p^*_{lk}(x',x)$ is its corresponding traction; u_k and p_k are the displacements and tractions in the boundary Γ, respectively, and $c_{lk}(x')$ is a jump term related to boundary geometry.

If there are no body forces present, (9) is reduced to the boundary-only equation,

$$c^i_{lk}(x')u^i_k(x') + \int_\Gamma p^*_{lk}(x',x)u_k(x) =$$

$$\int_\Gamma u^*_{lk}(x',x)p_k(x)\,\mathrm{d}\Gamma(x)\,. \qquad (10)$$

The basic idea behind BEM is to solve (10) numerically. To accomplish this, the model contour is discretized into N elements, where displacements $u_k(x)$ and tractions $p_k(x)$ are expressed in terms of the nodal values u^i_k and p^i_k by means of isoparametric interpolation functions. This process results in an algebraic system of equations from which the unknown nodal values of u^i_k and p^i_k can be recovered.

It should be noticed that (10) only involves integrals on $\Gamma(x)$. Consequently, a typical BEM formulation requires merely a boundary discretization and no domain discretization, the main advantage over FEM.

3.2 The dual reciprocity BEM (DRM) for two-dimensional thermoelasticity

Thermal effects (as much as body forces) were initially a restriction in the use of BEM, as they must be included in the formulation by means of a domain integral (see (9)), thus losing the method its original boundary-only character. Many different approaches have been developed to overcome this problem, among which DRM has become widely used. The basic idea behind this approach is to employ fundamental solutions and global approximation functions, as described in what follows.

Following Partridge and Sensale (1997), the effects produced by changes in temperature θ in elastic bodies can be represented by initial stresses σ^0_{jk} such that

$$\sigma^0_{jk} = \chi\theta\delta_{jk}\,, \qquad (11)$$

where $\chi = -2G\frac{1+\nu}{1-2\nu}\alpha$, so that (9) becomes

$$c^i_{lk}(x')u^i_k(x') + \int_\Gamma p^*_{lk}(x',x)u_k(x)\,\mathrm{d}\Gamma(x) =$$

$$\int_\Gamma u^*_{lk}(x',x)p_k(x)\,\mathrm{d}\Gamma(x) + \int_\Omega \chi\theta_{,k}(x)u^*_{lk}(x',x)\,\mathrm{d}\Omega(x) -$$

$$\int_\Gamma \chi u^*_{lk}(x',x)\theta(x)n_k(x)\,\mathrm{d}\Gamma(x)\,. \qquad (12)$$

In DRM, changes in temperature $\theta(x)$ are expressed in terms of known coordinate functions f^j, which are also temperature fields:

$$\theta \approx \sum_{j=1}^{N+L+A} f^j\beta^j\,, \qquad (13)$$

where β^j is a set of initially unknown coefficients, N points are placed on the contour and L in the domain and A augmentation functions are used to improve the approximation.

Next, a particular solution, $\hat{u}^j_{mk}$, to (8) corresponding to the generic function f^j, is found. Then, replacing (13) into (12) results in a boundary-only equation,

$$c^i_{lk}u^i_k + \int_\Gamma p^*_{lk}u_k\,\mathrm{d}\Gamma - \int_\Gamma u^*_{lk}(p_k - \chi\theta n_k)\,\mathrm{d}\Gamma =$$

$$\sum_{j=1}^{N+L+A}\left[c^i_{lk}\hat{u}^{ij}_{mk} + \int_\Gamma p^*_{lk}\hat{u}^j_{mk}\,\mathrm{d}\Gamma - \int u^*_{lk}\left(\hat{p}^j_{mk} - \chi f^j n_{mk}\right)\mathrm{d}\Gamma\right]\beta^j_m\,, \qquad (14)$$

where $\hat{p}^j_{mk}$ are the particular tractions corresponding to particular displacement solutions $\hat{u}^j_{mk}$. The procedure for numerical solution of (14) follows that described for (10).

The choice of approximation functions in (13) is somewhat arbitrary. Generally, a radial basis function is used, such as r, r^2, r^3 or $r^2\log(r)$. These have shown to interpolate only in the neighbourhood of a particular point (local behaviour), so that global functions are also needed. For these last, terms in the Pascal triangle or global sine Pascal triangle are often employed.

4 Implementation

The devised optimisation algorithm sticks to the following sequence:

i. An appropriate BEM mesh is generated for a reasonable initial design using quadratic isoparametric elements. In addition to the boundary nodes, internal points are also set. These are evenly distributed

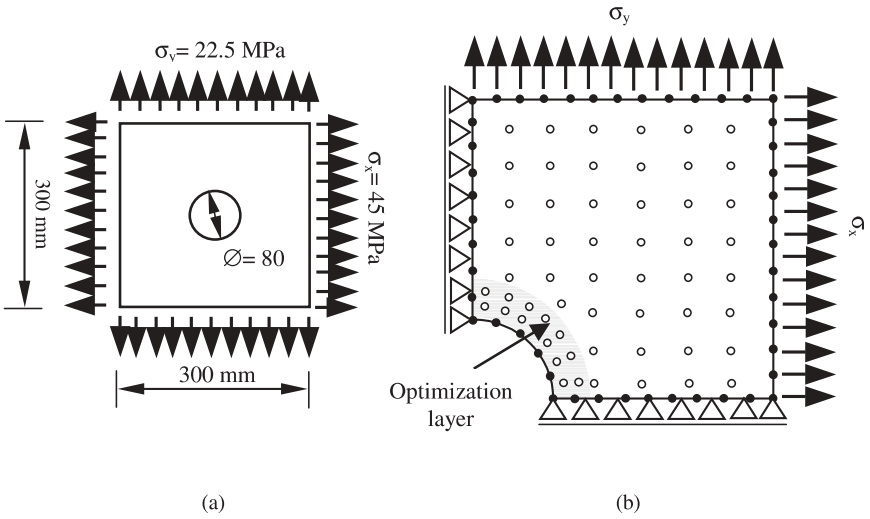

Fig. 1 Square plate with a circular hole under biaxial tension: (a) Model geometry and dimensions; (b) Discretization of the boundary element model: • boundary node, ○ internal point (note the concentration of internal points in the optimization layer)

over the complete model domain and over a thin layer along the optimisation boundary. Typically, 3–4 rows of optimisation internal points are used for this purpose (see Fig. 1).

ii. An appropriate stress reference value (σ_{ref}) is chosen.

iii. A stress analysis is performed using the elastic BEM formulation described in Sect. 3.1. Von Mises stresses are computed on the model boundary nodes and internal points.

iv. A thermal expansion analysis is performed using DRM (described in Sect. 3.2), with a temperature field θ given by (7). A nonzero temperature field is specified only on the optimisation boundary nodes and the internal points at the optimisation layer. This computation supplies the displacements at the optimisation boundary.

v. The geometry of the optimisation domain is updated using exponential spline interpolation. The spline interpolation of the new positions of the boundary nodes serves two purposes: to smooth the resultant geometry in order to avoid local wrinkles, which could act as artificial stress raisers; and to generate a good-quality BEM discretization (boundary nodes and internal points) for the new geometry.

Steps iii–v are repeated until von Mises stresses are reduced to the reference value or design limitations restrain further changes in the geometry.

5 Examples

5.1 Square plate with circular hole

This first example is that of a square plate with a circular, centred hole with remote loads applied in both directions, $\sigma_x = 45$ MPa and $\sigma_y = 22.5$ MPa (see Fig. 1). The aim of the process is to optimise the shape of the hole (note the thin layer of internal points parallel to the edge of the hole). Due to symmetry conditions, only one quarter of the problem is considered. The same problem was solved by Tekkaya and Güneri (1998) using BGM and FEM. Following their analysis, the reference stress was set to $\sigma_{ref} = 40$ MPa (nominal von Mises stress in the plate far from the hole). The adopted value for Young modulus was 525 MPa.

The evolution of the normalised von Mises stresses (σ_{vm}/σ_{ref}) obtained in this work is plotted for each loop in Fig. 2 as a function of the angle Θ (degrees) in the quarter of the hole. Also included as a reference are the results by Tekkaya and Güneri (1998) for the original circular geometry. It can be observed that, for the ini-

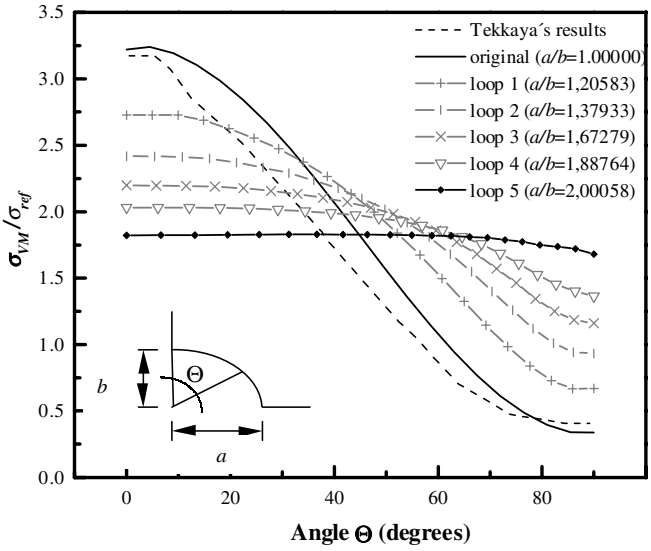

Fig. 2 Evolution of the normalized von Mises stresses along the quarter of a hole

tial geometry, the peak value corresponds to the vertical edge ($\Theta = 0°$), while the minimum coincides with the horizontal edge ($\Theta = 90°$), as the applied load in the y-direction is half the applied load in the x-direction ($\sigma_x/\sigma_y = 2$).

The optimum was achieved after five optimisation loops, similar performance to that of Tekkaya and Güneri (1998), who reached the optimal configuration after six loops using FEM. For the optimum configuration, the von Mises stresses are roughly uniform and equal to 70 MPa. It is worth mentioning that Muskhelishvili (in Savin 1961) analytically inferred that the minimum von Mises stress attainable in an infinite plate with a circular hole under biaxial tension is $\sigma_{vm}^{\text{minimum}} = \sigma_x + \sigma_y$, that is, $\sigma_{vm}^{\text{minimum}} = 67.5$ MPa for this example. This theoretical prediction is in very close agreement with the results shown in Fig. 2.

The legend in Fig. 2 includes the quotients of maximum over minimum dimensions of the hole, a/b, obtained after each loop. The value $a/b = 2.00058$ results after completion of the optimisation process. It is worth mentioning that Savin (1961) analytically predicted that, for the case of an infinite plate under biaxial tension, the circular hole would become elliptical and that the optimal geometry would be attained if and only if the quotient of maximum over minimum ellipse axis equals σ_x/σ_y, that is, 2 in this case. Once again, there is an excellent agreement between the results shown in Fig. 2 and the theoretical predictions.

It is easy to see in Fig. 2 that the initial peak stress at $\Theta = 0°$ is lowered through the swelling of that region, while the zone in which stresses were initially lower than the reference value (i.e. $\Theta = 90°$) shrinks, and consequently the stress level is increased.

5.2 Weld fillet

The second example consists of a weld fillet, illustrated in Fig. 3. A uniform stress $\sigma = 10$ MPa is applied in the horizontal direction. The optimisation boundary is indicated with a dotted line. Reference stress was chosen as $\sigma_{ref} = 10$ MPa. Thirty-six elements and a 198 internal points were used for the model discretization. The adopted value for Young modulus was 525 MPa. The same problem was solved by Li *et al.* (1999) by means of sensibility analysis with FEM.

Twenty-six loops were necessary in this case to attain an optimum configuration. Figure 4 illustrates the evolution of normalised von Mises stresses along the optimisation boundary, where the origin of the abscissas corresponds to position A, and 1 to position B (see Fig. 3). Note that, except in point A, the stress level on most of the optimisation boundary is below σ_{ref} for the original configuration. As the optimisation progresses, the structure shrinks, resulting in a general increase of the stress level. Except in the region close to point B, where stresses

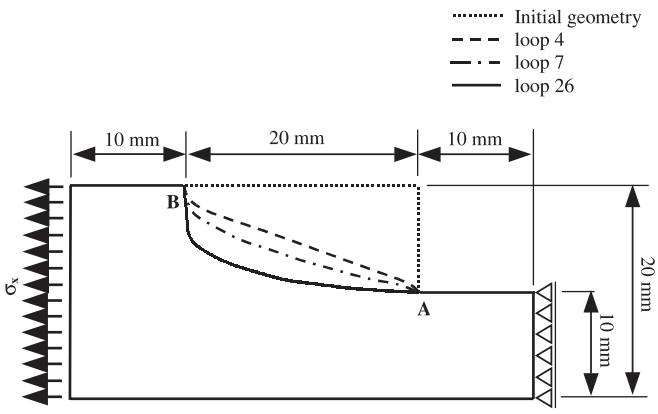

Fig. 3 Weld fillet: model geometry and boundary conditions, and evolution of the model geometry with the optimization process

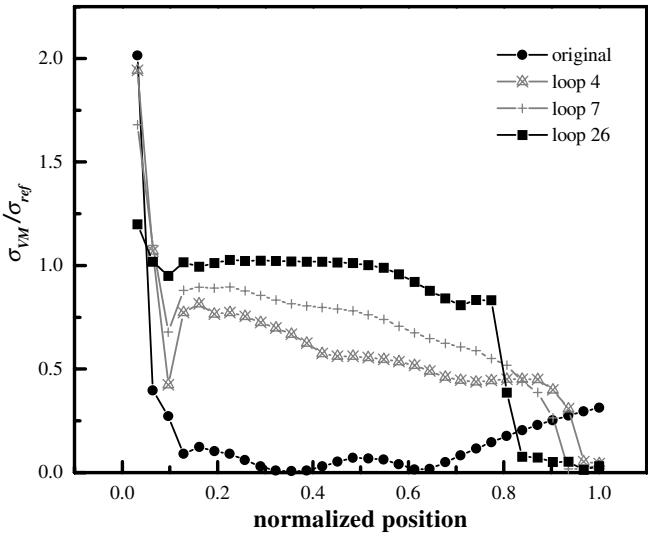

Fig. 4 Evolution of normalized von Mises stresses as a function of the normalized position in the optimization domain

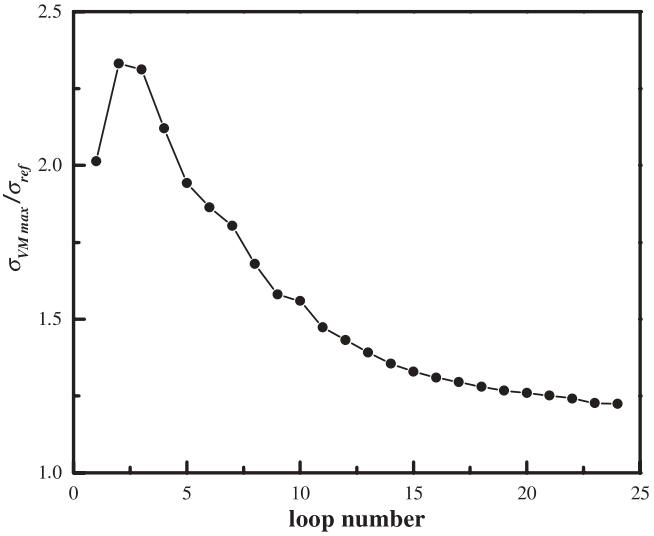

Fig. 5 Evolution of normalized maximum von Mises stresses as a function of the loop number

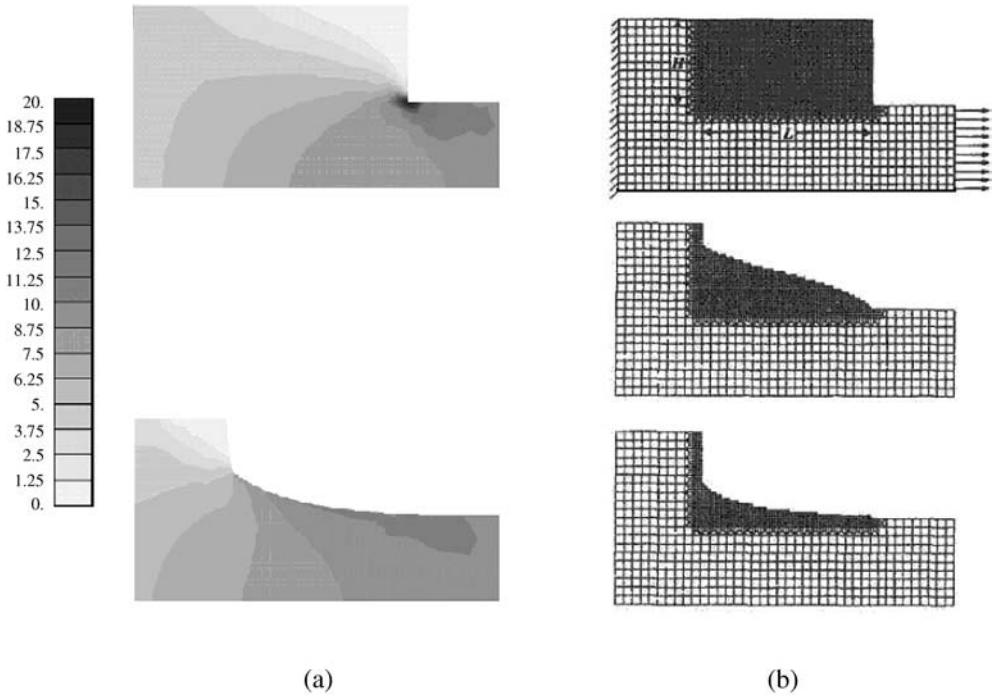

Fig. 6 (a) Distribution of von Mises stresses in the weld fillet for the initial and final configurations. (b) Qualitative results reported by Li *et al.*

can only be null, the final configuration shows a roughly uniform stress (approximately equal to reference stress), a fact that confirms that the optimisation procedure has been fulfilled.

Figure 5 presents maximum normalised von Mises stresses as a function of loop number. It shows how convergence is achieved after the optimisation has been carried out.

The evolution of the model shape is shown in Fig. 3 for selected loops. Consequently, Fig. 6 presents the stress maps corresponding to the initial and final geometries together with the results reported by Li *et al.* (1998). Note that both methods generate approximately the same final geometry. Unfortunately, Li *et al.* do not report the number of loops required to attain the optimum state; therefore, comparison of the performance of the methods is not possible.

6 Conclusions

A numerical evolutionary procedure for the structural shape optimisation of two-dimensional problems is presented in this work. The proposed procedure is based in BGM and was implemented using BEM. Two BEM formulations were employed in this work: the standard for two-dimensional elastostatics for the stress analysis, and DRM, which was used to model the swelling or shrinking of the material.

BEM has proven to be an excellent analysis technique in this kind of problem. The optimisation of a shape problem by BEM, as described in this work, did not require the discretization of the model domain, either for the stress or the swelling/shrinking analyses. This feature made the remeshing an easy task. In addition, BEM provided a continuum modelling of the interior of the problem domain without interior discretization. Very accurate values of both domain stresses and displacements could also be obtained when using BEM.

BGM has proven to be a simple and effective method to obtain homogeneously distributed surface stresses. Besides, the optimisation method based on it was easy to implement. The versatility of the proposed methodology was illustrated by a series of examples, and results were compared with those reported in the bibliography. Excellent results were obtained for all cases, showing the efficiency and effectiveness of the implementation.

Acknowledgements This work was founded by grant PICT 12-04586 of Agencia de Promoción Científica de la República Argentina and the Comisión Sectorial de Investigación Científica de la Universidad de la República de Uruguay.

References

Baron, M.R.; Yang, R.J. 1988: Boundary integral equations for recovery of design sensitivities in shape optimization. *J. AIAA* **26**(5), 589–94

Brebbia, C.A.; Domínguez, J. 1992: Boundary Elements: An Introductory Course. London: Computational Mechanics Publications, McGraw

Cai, R.; Cai, S.; Yang, X.; Lu, F. 1998: A novel method of structural shape optimization coupling BEM with an optimization method based on biological growth. *Struct. Opt.* **15**, 296–300

Chen, J.L.; Tsai, W.C. 1993: Shape optimization using simulated biological growth approaches. *J. AIAA* **31**(11), 2143–2147

Iancu, G. 1991: Spannungskonzentrationsminimierung dreidimensionaler elastischer Kontinua mit der FEM. Dissertation, Universität Karlsruhe

Iancu, G.; Schnack, E. 1988: Control of von Mises stress with dynamic programming. In: *Proc. of a GAMM-seminar*, Vol. 42. Berlin Heidelberg New York: Springer

Kane, J.H.; Saigal, S. 1988: Design-sensitivity of solids using BEM. *Eng. Mech.* **114**(10), 1703–22

Lewis, R.M.; Torczon, V.; Trosset, M.W. 2000: Direct search methods: then and now. *J. Comput. Appl. Math.* **124**(1), 191–207

Li, Q.; Grant, P.S.; Querin, O.M.; Xie, Y.M. 1999: Evolutionary shape optimization for stress minimization. *Mech. Res. Commun.* **26**(6), 657–664

Lucidi, S.; Sciandrone, M.; Tseng, P. 2002: Objective-derivative-free-methods for constrained optimization. *Math. Program* **92A**(1), 37–39

Mattheck, C. 1990: Design and growth rules for biological structures and their application to engineering. *Fatigue Fract. Eng. Mater. Struct.* **13**(5), 535–550

Mattheck, C.; Burkhardt, S. 1990: A new method of structural shape optimisation based on biological growth. *Int. J. Fatigue* **12**(3), 185–190

Mattheck, C.; Moldenhauer, H. 1990: An intelligent CAD-method based on biological growth. *Fatigue Fract. Eng. Mater. Struct.* **13**(1), 41–51

Mellings, S.C.; Aliabadi, M.H. 1995: Flaw identification using boundary element method. *Int. J. Num. Mech. Eng.* **38**, 399–419

Partridge, P.W.; Brebbia, C.A.; Wrobel, L.C. 1992: The Dual Reciprocity Boundary Element Method. Southampton, UK: Computational Mechanics

Partridge, P.W.; Sensale, B. 1997: Hybrid approximation functions in the dual reciprocity boundary element method. *Commun. Num. Mech. Eng.* **13**, 83–94

Sauter, J. 1993: A new shape optimisation method modelled on biological structures. *BENCH mark*. September

Sauter, J.; Bakhtiary, N.; Allinger, P.; Friedrich, M.; Mulfinger, F.; Müller, O.; Puchinger, M. 1996: A new approach for sizing, shape and topology optimization. In: *Proc. 1996 SAE International Congress and Exposition*

Savin, G.N. 1961: Stress Concentration Around Holes. Oxford, UK: Pergamon

Schnack, E. 1978: Ein Iterationsverfahren zur Optimierung von Spannungskonzentrationen. *VDI-Forsch Heft* 589

Schnack, E. 1988: A method of feasible direction with FEM for shape otpimization. In: Structural Optimization. Dordrecht, Boston, London: Kluwer, 299–306

Schnack, E.; Iancu, G. 1989: Shape design of elastostatic structures based on local perturbation analysis. *Struct. Opt.* **1**, 117–125

Schnack, E.; Iancu, G. 1991: Gradientless computer methods in shape optimization. In: Optimization of Structural Systems and Industrial Applications. Southampton, Boston: Computational Mechanics; London, New York: Elsevier, 363–376

Schnack, E.; Iancu, G. 1993: Optimization of large scale systems in elasticity. In: Optimization of Large Structural Systems, Vol. II. Dordrecht: Kluwer, 1073–1086

Schnack, E.; Spörl, U.; Iancu, G. 1988: Gradientless shape optimization with FEM. *Forschungsheft* **647**(88), 1–44

Spörl, U. 1985: Spannungsoptimale Auslegung elastischer Strukturen, Dissertation, Universität Karlsruhe

Tekkaya, A.E.; Güneri, A. 1998: Shape optimization with the biological growth method: a parameter study. *Eng. Comput.* **13**(8), 4–18

Trosset, M.W. 1997: I know it when I see it: toward a definition of direct search methods. *SIAG/OPT Views and News* **9**, 7–10